Protection Scheme Switch-Timing for Doubly-Fed Induction Generator during Fault Conditions

Jin Yang, *Student Member, IEEE*, John O'Reilly, *Senior Member, IEEE*, and John E. Fletcher

Abstract— This paper discusses the detailed switch-timing for converter protection schemes of doubly-fed induction generator (DFIG) to enhance the fault ride-through (FRT) capability. A new combined protection scheme with crowbar and series dynamic resistor (SDR) is used as proposed in former papers. Protection resistance values are calculated after the analysis of rotor fault current for practical application. The protection switching and rotor high current reduction performance are simulated with PSCAD/EMTDC. Fault ride-through performance including the reactive power supply, torque fluctuation and rotor speed with crowbar and series dynamic resistor are also shown. The proposed switch-timing scheme can reduce the time for fault ride-through, hence improving the DFIG fault ride-through performances.

Index Terms— Doubly-fed induction generator (DFIG), fault ride-through (FRT), converter protection switching, wind generation.

I. NOMENCLATURE

$\vec{v}$, $\vec{i}$, $\vec{\psi}$	Voltage, current and flux vectors.
V_s, V_r	Stator, rotor voltage amplitudes.
R_s, R_r	Stator, rotor resistances.
L_s, L_r, L_{ls}, L_{lr}	Stator, rotor self- and leakage inductances.
L_m	Magnetizing inductance.
ω_s, ω_r, $s\omega_s$	Synchronous, rotor and slip angular frequencies.
τ_s, τ_r, τ	Stator, rotor and combined time constants.
P_s, Q_s	Stator side active and reactive power.
s, r	Stator and rotor subscripts.
n	Nominal value subscript.

II. INTRODUCTION

THE doubly-fed induction generator (DFIG) is presently a very popular wind turbine generation system for large-scale wind farms. However, a significant disadvantage of DFIG is its vulnerability to grid disturbances and fluctuations because the stator windings are connected directly to the grid through a transformer and switchgear; the rotor-side is buffered from the grid via a partially-rated converter. So fault ride-through (FRT) capability is one of the basic requirements for wind farms with DFIGs. There are two aspects to fault ride-through: to continue power supply without breaking any part of the system and to resume normal operation after the clearance of faults.

As fault ride-through requirements have developed, an active crowbar protection scheme has emerged. This connects the crowbar when necessary and disables it to resume DFIG control. Existing crowbar control schemes fall into two categories: monitoring the rotor-side converter voltages and currents as the critical regulation reference [1]; using the DC-link bus voltage for crowbar triggering [2]. Some researchers have assumed that the crowbar was uneconomic and have avoided the use of crowbar control. They developed a new fault control strategy [3] or converter topology [4]. However, this makes the control system complex and increases the issues with control coordination between normal and fault operation.

In addition to the triggering and control issues, the blocking of the rotor-side converter by the switching-on crowbar is of concern. In a traditional system, the rotor-side converter is disconnected from the rotor when the crowbar is switched on. However, some studies have proposed keeping converter connected [1], [5]. With this kind of control, the resumption of normal operation can be immediate after fault clearance.

Another kind of power-electronic-controlled external resistor, which is connected to the rotor windings of the generator, is used to limit the rotor acceleration during a fault. This is called a braking resistor [6]. The purpose of the braking resistor is to balance the active power then improve generator stability during a fault. The advantages of a series dynamic braking resistor, when connected to the generation circuit, were studied in [7]. It was found that this enhanced the fault ride-through of a fixed speed wind turbine. Vestas (Denmark) use pitch-regulated variable rotor resistance to realize a quasi-variable-speed wind turbine (the OptiSlip® technology [8]). In [2], a braking resistor was inserted into the DC-link between the converters of DFIG; this acts as a dump load (or DC-chopper) to smooth the DC-link voltage during heavy imbalance of active power through the rotor-side and the grid-side converter. A similar resistor was proposed in [9] to enhance the fault ride-through capability of a permanent magnet synchronous generator with fully rated converter.

In former studies, a new topology and control strategy combining crowbar and series dynamic resistor (SDR) is proposed. In this paper, this protection scheme is used and presented in Section III and IV. The detailed switch-timing is discussed and simulated using PSCAD/EMTDC in Section V.

III. CONVERTER PROTECTION SCHEMES FOR DFIG

Existing protection systems use crowbars, DC-choppers (for DFIGs), and series braking resistors (for direct-driven fully-rated-converter generators). The traditional crowbar resistor

J. Yang and J. O'Reilly are with the Department of Electronics and Electrical Engineering, University of Glasgow, G12 8LT, UK (e-mail: j.yang@elec.gla.ac.uk, j.oreilly@elec.gla.ac.uk).

J. E. Fletcher is with the Department of Electronic and Electrical Engineering, University of Strathclyde, G1 1XW, UK (e-mail: john.fletcher@eee.strath.ac.uk).

bypasses the rotor-side converter when switched on. In [2], [9] a braking resistor (DC-chopper) is connected in parallel with the DC-link capacitor to limit the overcharge during low grid voltage. This protects the IGBTs from overvoltage and can dissipate energy, but this has no effect on the rotor currents.

In a similar way to the series braking resistor, a dynamic resistor can be put in series with the rotor (series dynamic resistor) and this limits the rotor over-current. Its operation is different from the crowbar. It can be controlled by a power-electronic switch. In normal operation, the switch is on and the resistor is bypassed; during fault conditions, the switch is off and the resistor is connected in series to the rotor winding.

In a rotor reference frame, the induction generator voltage can be expressed as $\vec{v}_r^r = \vec{v}_{r0}^r + R_r \cdot \vec{i}_r^r + \sigma L_r \dfrac{d\vec{i}_r^r}{dt}$. (1)

So the rotor equivalent circuit can be shown in Fig. 1 with all the protection schemes for a DFIG converter connected.
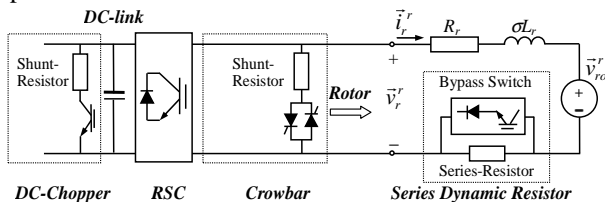

Fig. 1. DFIG rotor equivalent circuit with protections.

The distinctive series connection of the series dynamic resistor is advantageous for limiting the current magnitude directly. In addition, the limited current can reduce the charging current to the DC-link capacitor, hence helping avoid DC-link overvoltage. Moreover, with the proposed series dynamic resistor, the rotor-side converter does not need to be stopped. Two functions of a traditional crowbar are to bypass the converter and limit the current in the rotor windings. The first function is to protect the converter, while the second to protect the rotor windings. The obvious disadvantage of the bypassing function is that it turns the DFIG into a normal asynchronous machine. It then needs reactive power for excitation, so it will absorb reactive power from the grid that will exacerbate the grid voltage profile.

In the authors' former works, the series dynamic resistor and crowbar were combined and used for rotor-side converter protection: the shunt crowbar keeps its bypass function while the rotor current limit function is partially taken over by a series dynamic resistor. In this paper, the protection scheme is mainly based on the series dynamic resistor, combining the existing crowbar and DC-chopper. The crowbar is only used whenever needed during the beginning or the end of the fault as soon as possible to disable the rotor-side converter and further disconnect the wind turbine, if the series dynamic resistor cannot protect anymore because of deteriorating situations. At the same time, the DC-chopper is used for DC-link overvoltage limitation.

IV. SWITCH STRATEGY OF PROTECTION SCHEME

A. Fault Rotor Currents

From the above function analysis of crowbar and series dynamic resistor, in a time sequence, the latter should be switched on first. If the rotor current still increases the crowbar offers further protection. The switch-timing is related to the rotor current expression, which needs to be theoretically analyzed. (1) can be seen as the relationship between rotor voltage and current. When there is a disturbance on the stator side, assume that there is a sharp voltage amplitude change from V_1 to V_2. In [10] it was shown that $\vec{v}_{r0}^r$ can exceed the maximum voltage that the rotor-side converter can generate. In the same reference frame, the voltage is

$$\vec{v}_{r0}^r = V_2 \frac{L_m}{L_s} s e^{j\omega_s t} - \frac{L_m}{L_s}\left(\frac{1}{\tau_s} + j\omega\right)\frac{V_1 - V_2}{j\omega_s} e^{-t/\tau_s}. \quad (2)$$

This can be simplified by omitting $1/\tau_s$, which is very small:

$$\vec{v}_{r0}^r \approx V_2 \frac{L_m}{L_s} s e^{j\omega_s t} - \frac{L_m}{L_s} j\omega \frac{V_1 - V_2}{j\omega_s} e^{-t/\tau_s}. \quad (3)$$

So in the rotor reference frame

$$\vec{v}_{r0}^r \approx \frac{L_m}{L_s}\left[s V_2 e^{j\omega_s t} - (1-s)(V_1 - V_2)e^{-j\omega t} e^{-t/\tau_s}\right]. \quad (4)$$

(1) is a linear differential equation for $\vec{i}_r^r$ in the time domain, which can be solved and the final expression is

$$i_{ra}(t) = i_{DC} + i_{vr} + i_{vrf} + i_{vrn} \quad (5)$$

where the components are solved as:

$$i_{DC} = \left\{i_{ra}(t_0^-) - \frac{1}{\sigma L_r}\frac{\tau_r}{1+\tau_r^2(s\omega_s)^2}\left[V_r\cos\beta - V_s\frac{L_m}{L_s}s(1-p)\right]\right. \quad (6)$$

$$\left. -\frac{1}{\sigma L_r}V_s\frac{L_m}{L_s}(1-s)p\frac{\tau}{1+\tau^2\omega_r^2}\right\}e^{-\frac{t}{\tau_r}}$$

$$i_{vr} = \frac{V_r}{\sigma L_r}\left[\frac{\tau_r}{1+\tau_r^2\omega_r^2}\cos(s\omega_s t + \beta) + \frac{\tau_r^2\omega_r}{1+\tau_r^2\omega_r^2}\sin(s\omega_s t + \beta)\right] \quad (7)$$

$$i_{vrf} = -\frac{1}{\sigma L_r}V_s\frac{L_m}{L_s}s(1-p)\times \quad (8)$$

$$\left[\frac{\tau_r}{1+\tau_r^2(s\omega_s)^2}\cos(s\omega_s t) + \frac{\tau_r^2 s\omega_s}{1+\tau_r^2(s\omega_s)^2}\sin(s\omega_s t)\right]$$

$$i_{vrn} = \frac{V_s}{\sigma L_r}\frac{L_m}{L_s}(1-s)p\times\left[\frac{\tau}{1+\tau^2\omega_r^2}\cos(\omega_r t) + \frac{\tau^2\omega_r}{1+\tau^2\omega_r^2}\sin(\omega_r t)\right]e^{-\frac{t}{\tau_s}}. \quad (9)$$

The components are listed in TABLE I with frequency and decaying-time constant characteristics:

TABLE I FAULT ROTOR CURRENT COMPONENTS

Component	Frequency	Decaying-time constant
i_{DC}	DC	τ_r
i_{vr}	$s\omega_s$	-
i_{vrf}	$s\omega_s$	-
i_{vrn}	ω_r	τ_s

B. Switching Strategy

From the above over-current analysis a switch-timing strategy is devised.

1) Switch-on: The voltage change is not as abrupt as the current and can be shared by the series dynamic resistor. For the DC-link voltage, its change can be further reduced by the DC-chopper. Therefore, only rotor currents are monitored for series dynamic resistor and crowbar protections.

2) Switch-off: The protections themselves can be seen as disturbances. To avoid the protections switching frequently because of the high frequency component of rotor current, the switching off is delayed for about a period of the high frequency component, i.e. $t\_delay = 2\pi/(1-s)\omega_s$ after all the three-phase

currents decrease below the threshold value.

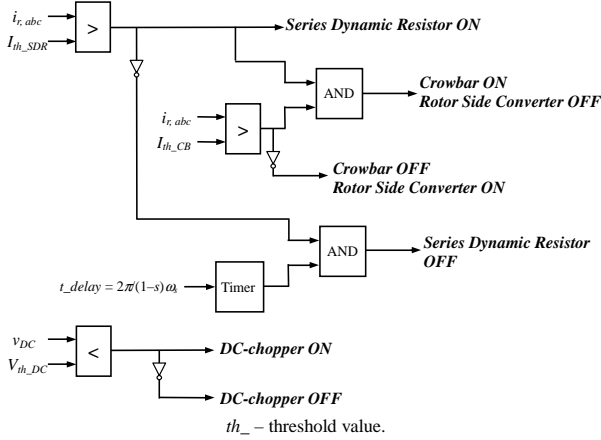The total switching strategy is shown in Fig. 2.

th_ – threshold value.

Fig. 2. The combined converter protection switching strategy.

C. Resistance Value Calculation

Resistance values are calculated for the most serious condition (with the highest peak current value): three-phase voltage dip up to 1.0p.u.. The rotor current expressions are (5) to (9). Due to the small stator resistance, the following approximations are made: $e^{-t/\varpi} \approx 1$; $\tau \approx \tau_r$. Then the current components are expressed in single trigonometric function, considering the amplitude of each component as the maximum current value:

$$i_{ra,\max} = i_{ra}(t_0^-) - \frac{1}{\sigma L_r} V_s \frac{L_m}{L_s} (1-s) \frac{\tau_r}{1+\tau_r^2 \omega_r^2}$$
$$+ \frac{V_r}{\sigma L_r} \frac{\tau_r}{\sqrt{1+\tau_r^2 \omega_r^2}} + \frac{1}{\sigma L_r} V_s \frac{L_m}{L_s} (1-s) \frac{\tau_r}{\sqrt{1+\tau_r^2 \omega_r^2}} \quad . \quad (10)$$

Also, the boundary conditions are

$$i_{ra,\max} \le I_{th\_SDR}; \ V_r \le V_{th\_RSC}. \quad (11)$$

Therefore, (10), (11) is an equation where τ_r can be solved. With the protection schemes

$$\tau_r = \frac{\sigma L_r}{R_r + R_{protection}} \quad (12)$$

Then the critical resistance value $R_{protection}$ can be calculated, including R_{SDR} and R_{CB}. Because the current-limiting function is mainly taken by series dynamic resistor, the critical criteria of crowbar resistance is the voltage across it within the rotor voltage limit, for its shunt connection: $R_{CB} \times i_{r,\max} \le V_{r,\max}$. So a smaller resistance can be taken from the total $R_{protection}$ as the crowbar resistance. For single crowbar protection, the double function means the resistance has to have both a lower and upper limit. The minimum value is related to the rotor winding over-current limit, while the maximum is set by the over-voltage on the converter terminals [11].

V. SWITCH-TIMING SIMULATION ANALYSIS

For the series dynamic resistor and crowbar, there are switching delays in the protection triggering process. The switching times mainly caused by the monitoring and device-switching delays. In practical applications, the switch time may be an issue, especially for serious fault protection and recovery when fast switching response is required e.g., some crowbar thyristor switches cannot interrupt the current before zero-crossing [8]. This will influence the protection performance. But

in former studies, the switching times of the protection switches were not considered. For serious fault condition, it is very important to rapidly disrupt and protect the wind power generation systems and quickly resume normal operation after the clearance of faults.

In the following simulations, the crowbar and series dynamic resistor power-electronic switches are simulated with IGBT components, which eliminate the zero-crossing delay. And switching times are considered by disabling the interpolation in PSCAD/EMTDC. This is used to solve the conflict between immediate switching-operation with simulation time step. The simulation time step is set as 20μs, so the actual switch time for IGBT is 20μs, which is enough for the IGBTs in applications (The normal switching time for power electronic controlled switches are short, commonly several μs [12]).

And also the detailed switch-timing needs to be clarified to make sure the efficiency of the protection scheme, as shown in Fig. 3. At almost the same time with fault happening (after the first time slot (a)), the series dynamic resistor is triggered. Then the system reaches into a new steady state. After a period, if the over-current still exists (if the fault deteriorates, or during the voltage recovery transient the rotor current goes high again), the crowbar can be switched in for a period (time slot (b)) in conjunction with the series dynamic resistor. The switching-out of crowbar makes the protection with only the series dynamic resistor in operation.

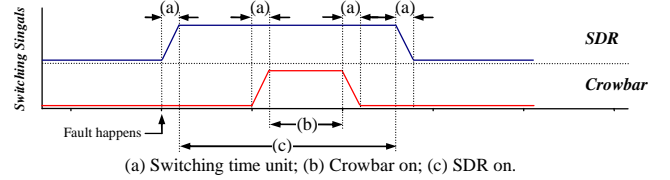(a) Switching time unit; (b) Crowbar on; (c) SDR on.

Fig. 3 Illustration of the protection switching sequence.

The protection scheme switch-timings are analysed by PSCAD/EMTDC simulations. The generator parameters are listed in the Appendix. The faults simulated are: (1) a three-phase voltage dip of 0.95p.u. for 0.2s; and (2) a three-phase voltage dip of 0.50p.u. for 0.5s.

The threshold values for calculating R_{SDR} and R_{CB} are set as $I_{th\_SDR} = 1.5$p.u., $I_{th\_CB} = 1.8$p.u.. Rotor slip is $s = -0.2$p.u. preceding the faults. From (10), (11), $\tau_r = 0.2041$p.u.; $R_{protection} = 0.59\Omega$. Then the selected resistance values are $R_{SDR} = 0.5\Omega$, $R_{CB} = 0.09\Omega$. The value of DC-chopper resistance is chosen as $R_{DCC} = 0.5\Omega$.

The primary protection is series dynamic resistor with converter in operation. Because this is related to the controller performance, the flux and slip angle without any protection is firstly shown to see the contribution of controller to the fault currents.

A. Fault-Occurrence Switch-Timings

Figs. 4 and 5 show the flux, slip angle and rotor current changes to the happening of a 0.5p.u. voltage dip for 0.5s without protection.
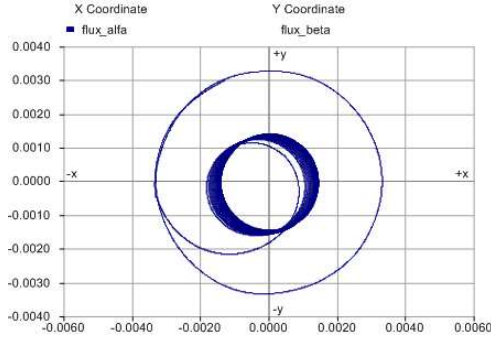
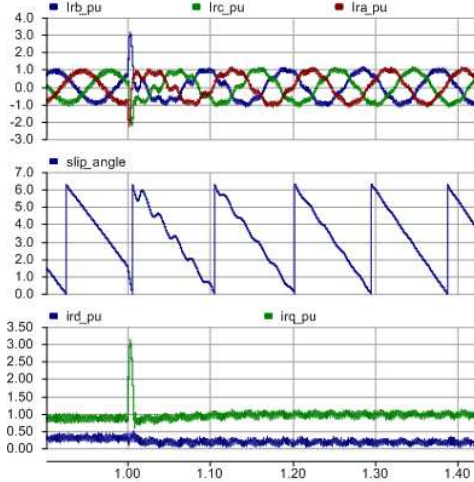Fig. 4. Stator flux during the occurrence of fault (voltage dip of 0.5p.u.).

Fig. 6. Stator flux during the recovery of fault (voltage dip of 0.5p.u.).

Fig. 5. Rotor currents and slip angle for fault occurrence (voltage dip of 0.5p.u.).
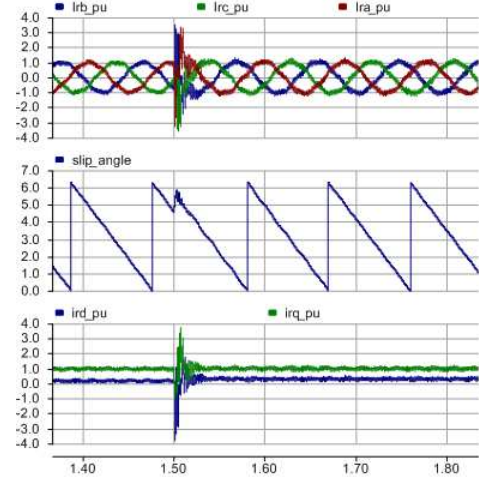
Fig. 7. Rotor currents and slip angle for fault recovery (voltage dip of 0.5p.u.).

The flux is basically in accordance with the analysis in [10], but the damping during the first few cycles of fault occurrence is faster because of different system parameters. In [10], the grid voltage dip is simulated by a controlled voltage source converter (VSC). It is very ideal with abrupt voltage amplitude change and no high frequency fluctuation.

The highest rotor phase current reaches around 3.0p.u. The controller and the fault condition make the final d-axis component of rotor currents have an abrupt change after the fault happens. The changing period is about dozens of ms.

B. Fault-Recovery Switch-Timings

Figs. 6 and 7 show the flux and rotor current change to the recovery of the corresponding 0.5p.u. voltage dip for 0.5s without protection.

The flux experiences a large fluctuation for several cycles until goes into the former steady state. To the authors' knowledge, there are no discussions about the flux performance during grid voltage recovery, in which a high fluctuation may influence the protection performance.

The slip angle change and the fluctuation make the final d- and q-axis components of rotor current experience abrupt change and high-frequency fluctuation corresponding to the fault recovery period.
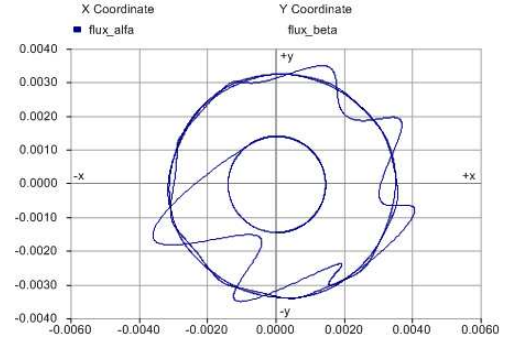
Now the series dynamic resistor is put in operation to see the switch-timing as shown in Fig. 8. From the simulation characteristics, the protection time is in accordance with the features of rotor currents, slip angle and rotor current d- and q-axis components. The total protection time is 0.02s + 0.024s = 0.044s, in which the switching time is 4×20μs = 80μs.
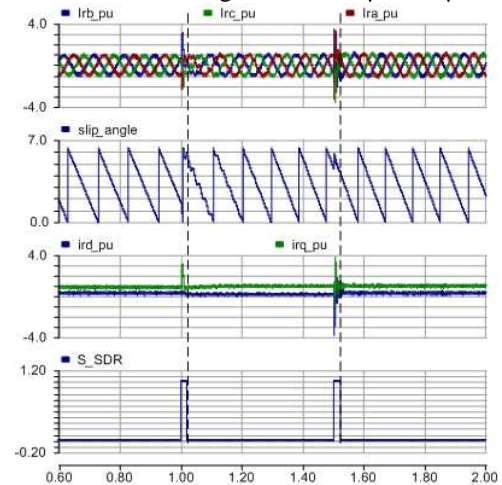

Fig. 8. Rotor currents and slip angle for fault recovery.

C. System Performance

The system performance including the stator active and reactive power, rotor speed, and electrical torque are shown in Fig. 9.
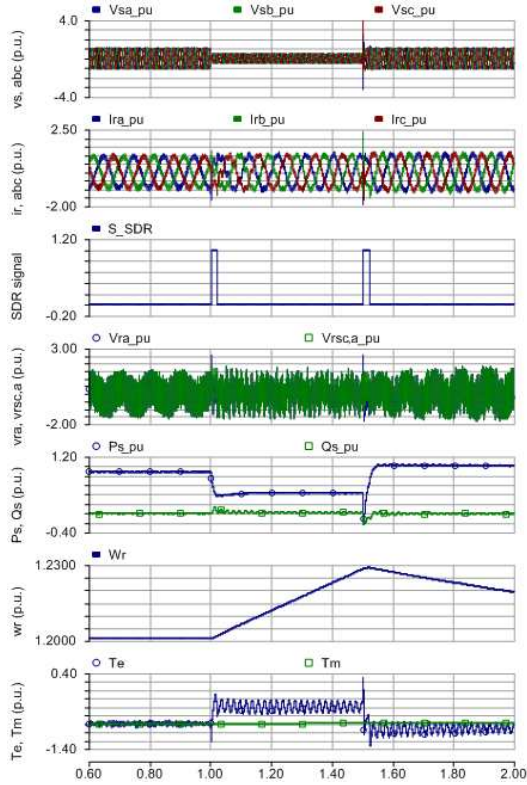
Fig. 9. With SDR protection, three-phase voltage dip of 0.5p.u. for 0.5 s.

Rotor speed increases until the fault is cleared. Large electrical torque fluctuations occur. In Fig. 9, with series dynamic resistor protection, the fault occurrence interruption is safely avoided, which also controls the rotor speed acceleration, increasing about 0.03 p.u..

Although there is no rotor voltage monitoring in the switching strategy, it is still limited effectively to the value before the fault because of the voltage share of series dynamic resistor. The rotor voltages display switching frequency components due to the pulse width modulation (PWM) of the rotor-side converter.

D. Switching of SDR and Crowbar

There is no need to switch crowbar protection in the above situation, which means the converter is in operation during the whole voltage dip period. But for a more serious fault, e.g. three-phase short-circuit, crowbar is required to further protect the converter from over-current.

Figs. 10 show the system response to a 0.95p.u. voltage dip for 0.2s with both series dynamic resistor and crowbar protection. The series dynamic resistor is switched in for 10 times to limit the rotor current. During the recovery of fault, crowbar is switched in for 5 times with series dynamic resistor connected because the rotor current keeps increasing. The simulation results show that with series dynamic resistor protection, the fault occurrence interruption period is safely avoided, while crowbar is helpful for protection during fault recovery: The rotor current amplitude is limited within 1.5p.u., as required. This also restricts the DC-link voltage increase (less than 0.05p.u. in Fig. 10). The DC-chopper is not even needed to function. The former big torque fluctuation is avoided as well; hence effectively restrain the rotor speed increase, from 1.2p.u. to 1.207p.u. (only 0.007p.u.).
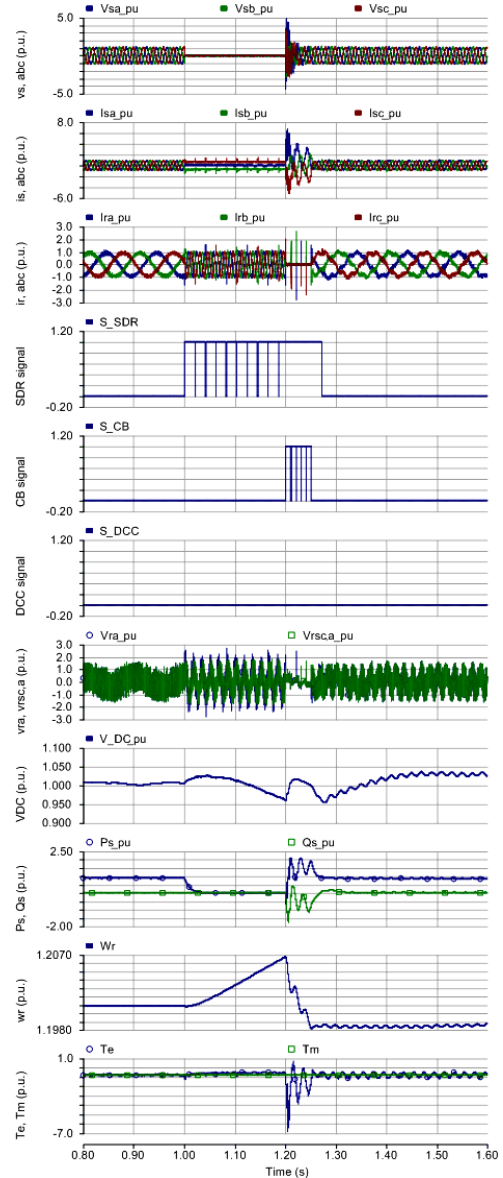

Fig. 10. With converter protections, three-phase voltage dip of 0.95p.u. for 0.2 s.

Both of the above two situations show that with series dynamic resistor in connection, reactive power and electrical torque fluctuations during the fault are existed. However, for crowbar protection, they are much heavier. The reactive power and electrical torque ripples are larger with series dynamic resistor protection compared to crowbar protection. This is due to the higher resistance in rotor winding and DFIG control system performance during faults, which needs further exploration.

More importantly, the series dynamic resistor has a much smaller impact than the crowbar, especially during switching-off. Improper crowbar switch-off strategy (without the coordination of controller reference settings [1]) can cause frequent switchings which will deteriorate the fault recovery. This can also be seen from the comparison of voltage recovery in Figs. 9 and 10. Without crowbar switching, the voltage recovery for the two-phase short-circuit is with little fluctuation. On the other hand, all the series dynamic resistor switching has little influence on the system response, due to its minor impact on the system – just a resistance change in the rotor circuit.

VI. Conclusion

From the angle of reducing DFIG fault ride-through time, this paper discusses the switching time issue with series dynamic resistor and crowbar combined protection scheme. This is advantageous for the resume of normal operation and the protection of the generation system. With the proposed switching scheme, it is faster to resume normal operation and the affected time is effectively shortened, with improved fault ride-through performances.

VII. Appendix

TABLE II Generator Parameters

Parameter	Value	Parameter	Value
Rated power P_n	2 MW	Ratio N_s/N_r	0.63
Rated stator voltage V_{sn}	690 V	Inertia constant H	3.5 s
Rated frequency f_s	50 Hz	Pole pair no. P_p	2
Stator leakage inductance L_{ls}	0.105 p.u.	Stator resistance R_s	0.0050 p.u.
Rotor leakage inductance L_{lr}	0.100 p.u.	Rotor resistance R_r	0.0055 p.u.
Magnetizing inductance L_m	3.953 p.u.		

VIII. References

[1] J. Morren, and S.W.H. de Haan, "Ridethrough of wind turbines with doubly-fed induction generator during a voltage dip," *IEEE Trans. Energy Convers.*, vol. 20, no. 2, pp. 435-441, Jun. 2005.

[2] I. Erlich, J. Kretschmann, J. Fortmann, S. Mueller-Engelhardt, and H. Wrede, "Modeling of wind turbines based on doubly-fed induction generators for power system stability studies," *IEEE Trans. Power Syst.*, vol. 22, no. 3, pp. 909-919, Aug. 2007.

[3] D. Xiang, R. Li, P. J. Tavner, and S. Yang, "Control of a doubly fed induction generator in a wind turbine during grid fault ride-through," *IEEE Trans. Energy Convers.*, vol. 21, no. 3, pp. 652-662, Sep. 2006.

[4] A. Gaillard, S. Karimi, P. Poure, S. Saadate, and E. Gholipour, "A fault tolerant converter topology for wind energy conversion system with doubly fed induction generator," in *Proc. 12th Eur. Conf. Power Electronics and Applications*, Sep. 2-5, 2007.

[5] A. Dittrich and A. Stoev, "Comparison of fault ride-through strategies for wind turbines with dfim generators," in *Proc. 11th Eur. Conf. Power Electronics and Applications*, Dresden, Germany, Sep. 11-14, 2005.

[6] W. Freitas, A. Morelato, and W. Xu, "Improvement of induction generator stability using braking resistors," *IEEE Trans. Power Syst.*, vol. 19, no. 2, pp. 1247-1249, May 2004.

[7] A. Causebrook, D. J. Atkinson, and A. G. Jack, "Fault ride-through of large wind farms using series dynamic braking resistors (March 2007)," *IEEE Trans. Power Syst.*, vol. 22, no. 3, pp. 966-975, Aug. 2007.

[8] J. M. Carrasco, E. Galván, R. Portillo, L.G. Franquelo, and J.T. Bialasiewicz, "Power electronic systems for the grid integration of wind turbines, " in *Proc. 32nd Annual Conf. IEEE Industrial Electronics – IECON 2006*, pp. 4182-4188, Nov. 2006.

[9] J. F. Conroy and R. Watson, "Low-voltage ride-through of a full converter wind turbine with permanent magnet generator," *IET Renew. Power Gener.*, vol. 1, no. 3, pp. 182-189, 2007.

[10] J. López, P. Sanchis, X. Roboam, and L. Marroyo, "Dyanmic behavior of the doubly fed induction generator during three-phase voltage dips," *IEEE Trans. Energy Convers.*, vol. 22, no. 3, pp. 709-717, Sep. 2007.

[11] J. Morren and S. W. H. de Haan, "Short-circuit current of wind turbines with doubly fed induction generator," *IEEE Trans. Energy Conversion.*, vol. 22, no. 1, pp. 174-180, Mar. 2007.

[12] S. Castagno, R. D. Curry, and E. Loree, "Analysis and comparison of a fast turn-on series IGBT stack and high-voltage-rated commercial IGBTs," *IEEE Trans. Plasma Science*, vol. 34, no. 5, pp. 1692-1696, Oct. 2006.